

Fatigue behavior of sylramic-iBN/BN/CVI SiC ceramic matrix composite in combustion environment

D. J. Bertrand^{1,2} · V. Sabelkin¹ · L. Zawada² · S. Mall¹

Received: 29 April 2015 / Accepted: 25 July 2015 / Published online: 5 August 2015
© Springer Science+Business Media New York (outside the USA) 2015

Abstract Fatigue behavior of Sylramic-iBN/BN/CVI SiC CMC was investigated under tension–tension fatigue using a test facility which simulated simultaneously both loading and combustion conditions of hot-section components of gas turbine engines. Combustion environment was created using a high-velocity oxygen fuel gun to impinge combustion flame on one side of specimen subjected to fatigue to simulate the real situation. The flame-impinged surface of specimen was heated to average temperature of 1250, 1350, or 1480 °C. Ultimate tensile strength of CMC was about 270 MPa at 1480 °C under combustion environment. Fatigue life diagram was established at stress ratio of 0.1 and frequency of 1 Hz. The CMC survived up to 25 h at 46 and 33 % of ultimate tensile strength under combustion at 1250 and 1350 °C, respectively. However, it could not survive 25 h at 1480 °C under combustion fatigue environment even with no stress on the specimen due to degradation/erosion of the material. Microscopic analysis of fracture surface showed oxidation of BN interface, which was more on flame side than other side. Fracture surfaces showed oxide formation over matrix, fibers, and/or

fiber/matrix interphase causing embrittlement and there-after failure of CMC.

Introduction

Materials with higher strength-to-weight ratio and capable of operating at elevated temperatures are needed to improve efficiency and thrust-to-weight ratio in military and civilian gas turbine engines. Ceramic matrix composites (CMC) have been identified as the enabling materials for the next generation of advanced gas turbine engines due to their better specific properties at temperatures beyond the operating temperatures of conventional nickel-base superalloys [1, 2]. Among CMCs, silicon carbide (SiC) fibers in SiC matrix (i.e., SiC/SiC)-based systems have capability to withstand higher temperature [2]. However, one limitation of the SiC/SiC system is that it is prone to oxidation that can cause embrittlement and degradation of the performance over time under oxidizing environments. This has motivated various experimental studies involving different environmental impacts on these materials. The effects of moisture environments on the oxidation of SiC and SiC/SiC CMCs have received a great deal of attention [3–8]. The presence of the water vapor enhances the growth rate of SiO₂ on SiC at elevated temperatures which leads to accelerated rates of SiC recession [3–8]. Effects of moisture on the BN fiber coatings and SiC/SiC composites have been reported [9–18]. These studies have shown that these CMCs are degraded in the presence of moisture which depends upon the level of moisture, temperature, and amount of matrix cracking (or applied stress level).

CMCs are exposed to the different mechanical loads (e.g., fatigue, creep, etc.) under combustion environment during

The views expressed in this article are those of the authors and do not reflect the official policy or position of the United State Air Force, Department of Defense, or the U.S. Government.

✉ S. Mall
Shankar.Mall@afit.edu

¹ Department of Aeronautics and Astronautics, Air Force Institute of Technology (AFIT/ENY), Wright-Patterson AFB, Bldg. 640, 2950 Hobson Way, Dayton, OH 45433-7765, USA

² Materials & Manufacturing Directorate, Air Force Research Laboratory, Wright-Patterson AFB, Dayton, OH 45433-7817, USA

their usage in gas turbine engines. With this perspective, CMC coupons have been subjected to a set of combustion environmental conditions for a prescribed duration in a burner rig test facility, and thereafter the coupons have been evaluated at room temperature for the post-combustion mechanical properties such as residual tensile strength, weight loss, oxidation of fiber/matrix interphase, damage mechanisms etc. [19–21]. This sequential approach has provided the understanding of the effects of a given combustion environment with the set time of exposure, but it does not represent a realistic situation of a load-carrying structural component in a gas turbine engine. There have been also limited numbers of investigations of CMCs when subjected to the simultaneous applications of mechanical load and combustion environment [22–25]. Previous studies have investigated a melt-infiltrated woven ceramic matrix composite (CMC) consisting of a silicon carbide (SiC) matrix reinforced by boron nitride (BN)-coated Hi-Nicalon type-STM SiC fiber, Hi-Nic-S/BN/SiC under the tension–tension fatigue condition in a combustion environment representative of those experienced by hot-section components such as turbine blades and vanes in modern gas turbine engines [22, 24]. The burner rig fatigue data and fracture surfaces were analyzed for the effects of oxidation on life, failure, and damage mechanisms. These test results were also compared with those obtained from similar fatigue tests performed in a standard furnace under laboratory air environment. Fatigue life in the combustion condition was lower by an order of magnitude in comparison to the isothermal furnace due to a thermal gradient caused by the flame and enhanced oxidation from the moisture which is significantly higher in a typical combustion environment. In a follow-up study, the fatigue behavior of two versions of Hi-Nicalon Type-STM/BN/SiC CMCs was investigated in a combustion environment [23]. The first version was manufactured by slurry casting process using woven fiber architecture and the matrix was densified by melt-infiltration (MI) of silicon. The other system was a cross-ply laminate prepared by a traditional lamination process from unidirectional prepreg followed by the MI processing. The prepreg version exhibited better fatigue performance and less oxidation in comparison to the slurry cast version.

The present study involves the characterization of a newer version of SiC/SiC CMC when subjected to the tension–tension fatigue condition under a simulated combustion environment. This version of SiC/SiC CMC is projected to have higher temperature capability (i.e., greater than 1250 °C) unlike the previous SiC/SiC versions capable of withstanding temperature up to 1250 °C [22–24]. Therefore, the objective of the present study was to characterize the tension–tension combustion fatigue behavior of this newer version of SiC/SiC CMC at temperatures greater than 1250 °C.

Experimental procedure

Material and specimen details

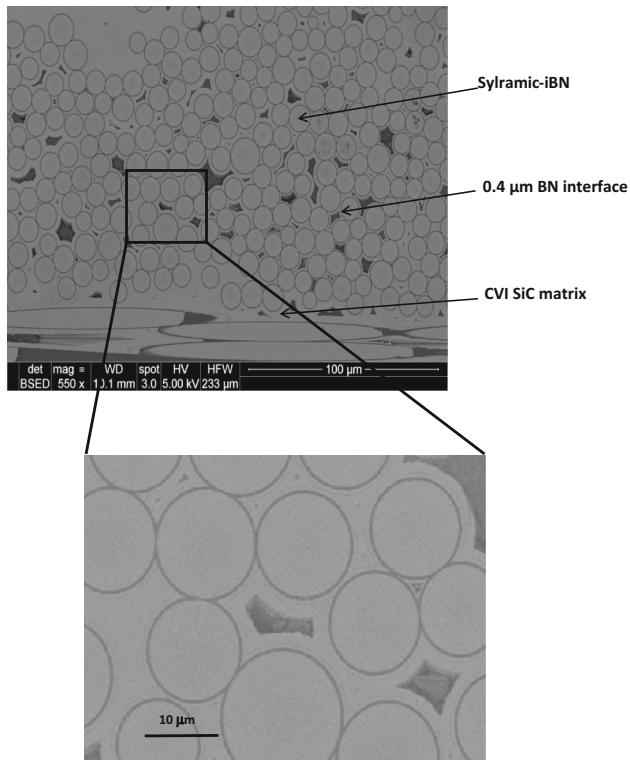
The CMC of this study was Sylramic-iBN/BN/CVI SiC CMC. It contained 8HSW of woven Sylramic fibers with in situ BN layer and then coated with BN interface. Thereafter, SiC matrix was built around the fibers by the chemical vapor infiltration (CVI) method. The CMC system of the present study had twice the ends per inch along the longitudinal direction compared to the transverse direction (i.e., 2:1 unbalanced lay-up). The fiber volume fraction was about 35 %. This CMC material was produced by Rolls-Royce High Temperature Composites. Dog-bone-shaped coupons were machined from a flat panel. A specimen is shown in Fig. 1. The nominal width in the gage section and thickness was 10 and 2 mm, respectively. A cross-sectional view (transverse to the loading direction) of the tested CMC is shown in Fig. 2 to show the pristine internal state of material. The porosity is evident as expected due to CVI process. Further, several fibers are in physical contact with each other; however the BN coating is uniform and continuous all the way around the fibers.

Combustion-load test setup

A combined combustion and loading test facility was used which was capable of subjecting the specimens to various mechanical loading conditions while simultaneously being exposed to a combustion environment. The combustion environment was produced using a commercially available Sulzer Metco Diamond Jet High-Velocity Oxygen Fuel (HVOF) spray gun system. The HVOF spray gun uses oxygen and propane to create combustion conditions with pressurized air used for cooling the nozzle. The conditions produced by the flame gun were set to be representative of the operating conditions inside a typical gas turbine engine. Since propane has similar reaction characteristics to aviation fuel such as JP-8 [24], it was used as the fuel in creating the combustion conditions for this study. The flow rates were 220–230 scfh of O₂, 50–75 scfh of C₃H₈, and 364–368 scfh of air. The flow rates were adjusted as necessary within these ranges to achieve the target specimen surface temperature. Gas velocity was measured which was a Mach of approximately 0.5 [25]. Figure 3 shows the flame gun in action with a specimen installed in a servo hydraulic test machine.

For the tests conducted under combustion condition in this study, fatigue load was applied. The fatigue loading profile was of sinusoidal type at 1 Hz with a stress ratio, $R = 0.1$ where

$$R = \sigma_{\min} / \sigma_{\max}, \quad (1)$$

Fig. 1 Test specimen**Fig. 2** Close-up view of polished cross-section of un-tested specimen and further magnified view

where σ_{\max} and σ_{\min} are maximum and minimum applied fatigue stress during a cycle, respectively. One of the challenges was to keep the MTS grips being getting hot during the test at the elevated temperatures of this study. This was accomplished using multiple techniques of insulating the grips as well as actively cooling them. A chilled water system was used to circulate cool water to the grips to actively cool them. Multiple layers of aluminum oxide-based insulation were installed to protect the grips from the combustion environment. Additionally, compressed air at 130 kPa was directed at the top and bottom ends of the specimen to deflect hot gases from the grips.

To record the temperature of specimens during a test, a FLIR SystemsTM ThermaCamTM P640 infrared camera system was used since the environment was not ideal for the direct temperature measurement by a thermocouple.

Temperature of the specimen was controlled by adjusting the distance between the flame gun and the specimen. As the flame was moved closer to the CMC to achieve 1480 °C, the flame would directly impinge on the specimen. Temperature varied from a point to point due to uneven surface texture of the CMC. Therefore, the average temperature over a small area at the center of a specimen was used as the target temperature, and this area was either a circle (17 mm²) or a square (21 mm²) region as shown in Fig. 4, and both provided the value within ± 30 °C. An IR image was recorded every ten minutes in each test. Further details for fatigue tests in combustion environment are provided in Kim et al. [24] including calibration of temperature measurement. As mentioned earlier, the objective of the present study was to characterize the tension–tension fatigue behavior of CMC at temperatures at and greater than 1250 °C. Therefore, the three test temperatures were selected: 1250, 1350, and 1480 °C. Fatigue tests were run up to the maximum of 25 h (or 90,000 cycles) if the specimen survived. This maximum test duration of 25 h (90,000 cycles) was chosen to represent the realistic exposure time at maximum temperature of some aerospace turbine hot-section components [24].

Results and discussion

Monotonic tension

Monotonic tension test was performed in the burner rig test setup (i.e., under combustion condition) where the surface of the test specimen was heated to an average temperature of 1480 °C. Specimen was first heated by the combustion flame to stabilize the temperature for about 10 min, and then tested under monotonic tension. The loading rate was 20 N/s. The applied load and cross-head displacement were recorded during this test due to the difficulties in attaching a displacement or strain gage to the specimen in the harsh environment produced by the combustion flame. The stress versus displacement relationship from this test is shown in Fig. 5. The ultimate tensile strength of the CMC material in the combustion environment was found to be 274 MPa which is approximately 15 % lower than the UTS

Fig. 3 Combustion flame gun on specimen subjected to fatigue

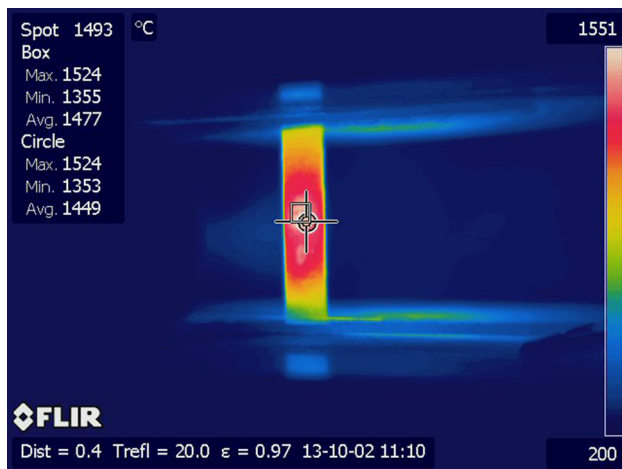
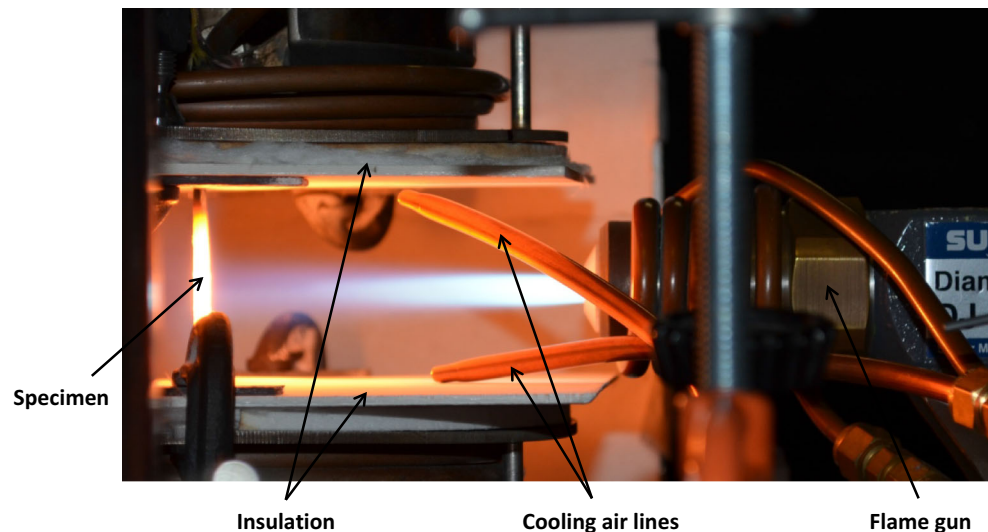


Fig. 4 IR camera image during combustion fatigue test

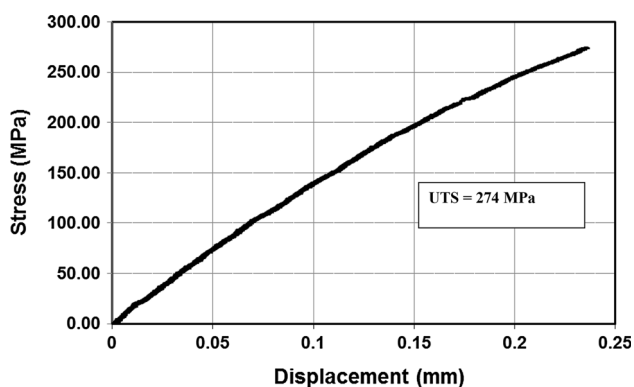


Fig. 5 Tensile stress versus displacement curve for Syramic-iBN/BN/SiC in combustion environment at 1480 °C

(323 MPa) at the same temperature in laboratory ambient environment. The laboratory air tension test data were provided by Rolls-Royce High Temperature Composites, Inc.

The reduction in ultimate tensile strength of the CMC in the combustion environment can be due to the thermal stresses when compared to uniform heating in standard furnace as well as due to the damage from the combustion environment. A thermal gradient was present in the specimen when subjected to the combustion flame heating on one side of the specimen. Figure 6 shows the typical temperature distribution along the longitudinal and transverse directions on the front and back faces of the specimen. There was about a difference of 200 °C between front and back faces. The thermal gradient will introduce thermal stresses within the material that is not experienced during the uniform heating in a standard furnace and would contribute toward the reduction in the ultimate tensile strength.

Fatigue

Applied maximum stress versus number of cycle (S–N) relationships obtained from tension–tension fatigue test condition under combustion environment at three test temperatures are compared in Fig. 7. The applied maximum stress ranged from 30 to 77 % of the ultimate tensile strength (274 MPa) under combustion environment. The run-out condition in the fatigue combustion tests was set to 90,000 cycles (i.e., 25 h). The fatigue life decreased with increasing applied stress and temperature. Specimens tested at the same maximum stress level display a decrease in fatigue life with increasing temperature. However, the decrease was minimal between 1250 and 1350 °C, but substantially greater at 1480 °C. For example, the fatigue lives at the applied maximum stress level of 125 MPa were >90,000, ~70,000, and ~13,000 cycles at 1480, 1350, and 1250 °C, respectively. The maximum stress levels for the run-out condition of 25 h were 125 and 90 MPa, or about 46 and 33 % of the ultimate tensile strength

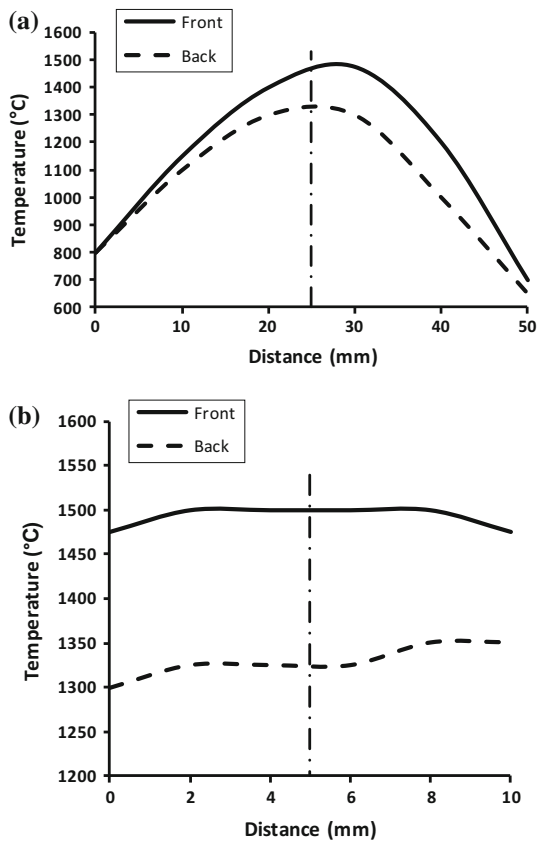


Fig. 6 Temperature distribution along a longitudinal direction and **b** transverse direction of the specimen (center of the specimen in longitudinal or transverse direction is shown by dotted line)

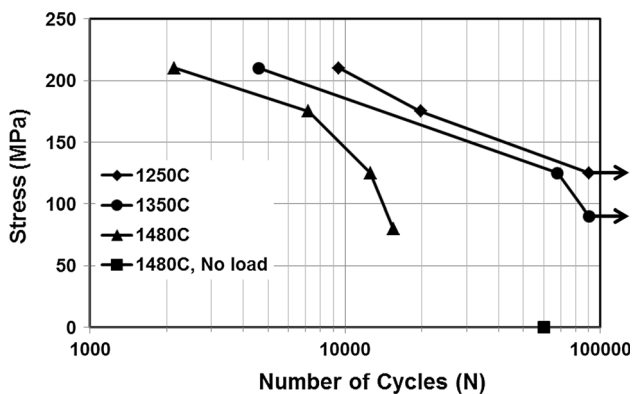


Fig. 7 Applied maximum stress versus cycles to failure at 1250, 1350, and 1480 °C

(274 MPa) under combustion environment at 1250 and 1350 °C, respectively. However, no run-out condition at 1480 °C could be achieved as elaborated next.

Material loss

The major reason for not achieving the run-out condition at 1480 °C was the physical loss of cross-sectional area, i.e.,

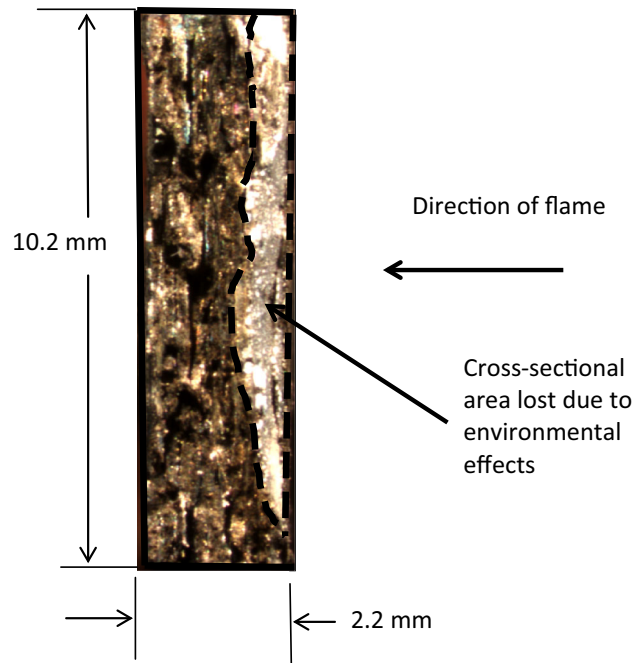


Fig. 8 Optical image showing the loss of cross-sectional area in the thickness direction for the specimen tested at 1480 °C and 125 MPa maximum stress

material loss. Figure 8 is an optical image showing the loss of area in the specimen tested at 1480 °C and 125 MPa. This view shows the loss of material in the thickness direction of the specimen exposed to combustion flame. Table 1 shows the measured cross-sectional areas of two specimens tested at 1480 °C before and after the fatigue test to illustrate this further. The first specimen was subjected to a maximum cyclic stress of 125 MPa and the second specimen was subjected to a maximum cyclic stress of 80 MPa. These stresses are based on the initial cross-sectional area, i.e., at the start of test. However, the stress experienced by the specimen increased as cross-sectional area decreased due to the recession of the material. When the loss of cross-sectional area is taken into account, the actual maximum stresses at the time of failure were 20 and 61 % higher than the initial stress of 125 and 80 MPa specimens, respectively. Thus, loss of material enhanced the applied stress causing premature failure due to overload. Therefore, applied stress versus cycles to failure relationship at 1480 °C in Fig. 7 should be looked with this perspective. A fractured specimen with material loss is shown in Fig. 9.

To investigate the material loss further, a specimen was tested under the combustion environment without any applied fatigue load at 1480 °C. There was also significant material loss in this case. This specimen survived only up to 16.7 h, and had the largest amount of material loss in this study due to maximum exposure time under the

Table 1 Cross-sectional area before and after failure

Specimen	Initial cross-sectional area (mm ²)	Cross-sectional area at failure (mm ²)	Engineering maximum stress (MPa)	Actual maximum stress (MPa)
1480 °C, 125 MPa, 3.5 h	22	18	125	150
1480 °C, 80 MPa, 4.3 h	26	16	80	129

combustion environment. This failure time is equivalent to about 60,000 cycles with frequency of 1 Hz. So, these data are also shown on the fatigue life diagram (Fig. 7) for the sake of comparison even though it was not subjected to fatigue. Figure 10 shows the series of IR photographs of this specimen at different intervals during the test depicting the progression of the damage due to the combustion environment as well as temperature field on the width face of the specimen. This figure also shows the erosion along the thickness direction obtained from an optical camera. Thickness measurements were taken at three locations on the flame-impinged side of the specimen, and these data are

shown in Fig. 11. Overall, a linear time rate of recession can be approximated, i.e., material eroded at the almost constant rate over the test duration. An average recession rate at three locations was calculated, and it was about 0.18 mm/h. A previous study has investigated the recession of pure SiC that has shown that there are the two major contributors to the recession of SiC in combustion conditions. These are oxidation and vaporization [26]. SiC reacts with O₂ to form SiO₂ scale which limits the recession of SiC. The presence of H₂O increases the permeation of O₂ through the SiO₂ and increases the volatilization of SiO₂ through the reaction in the following way:

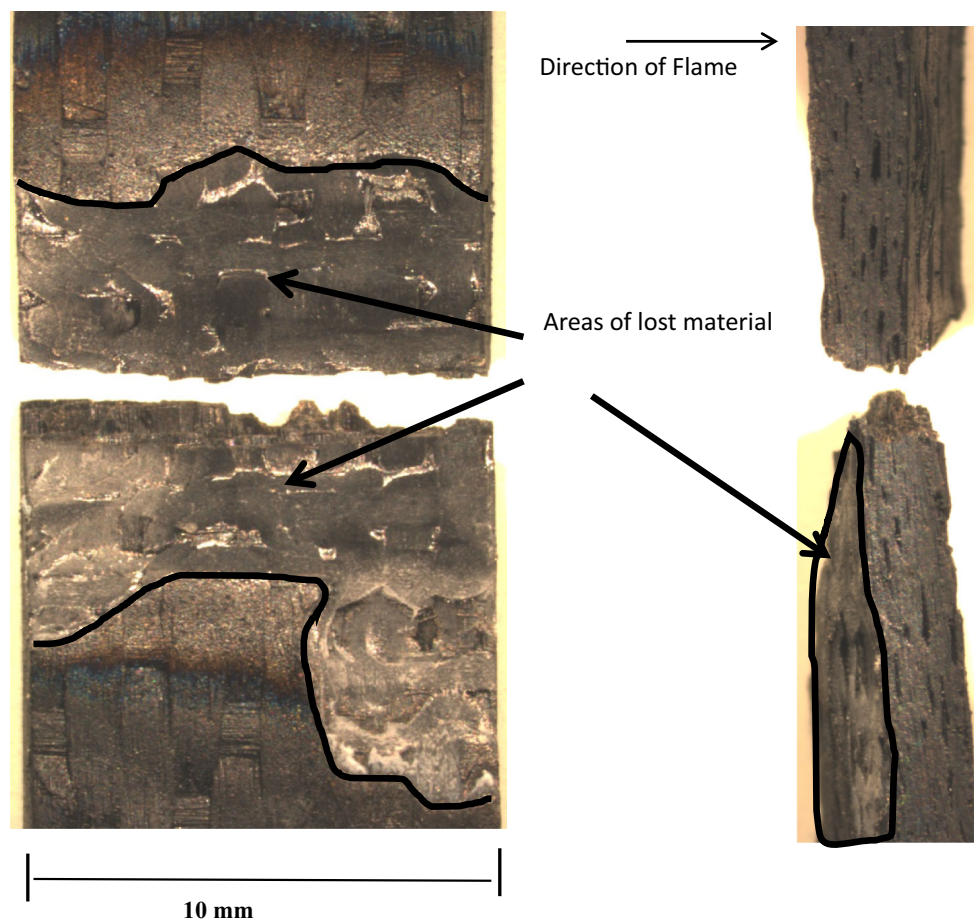
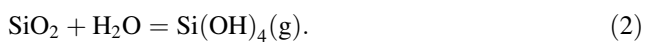
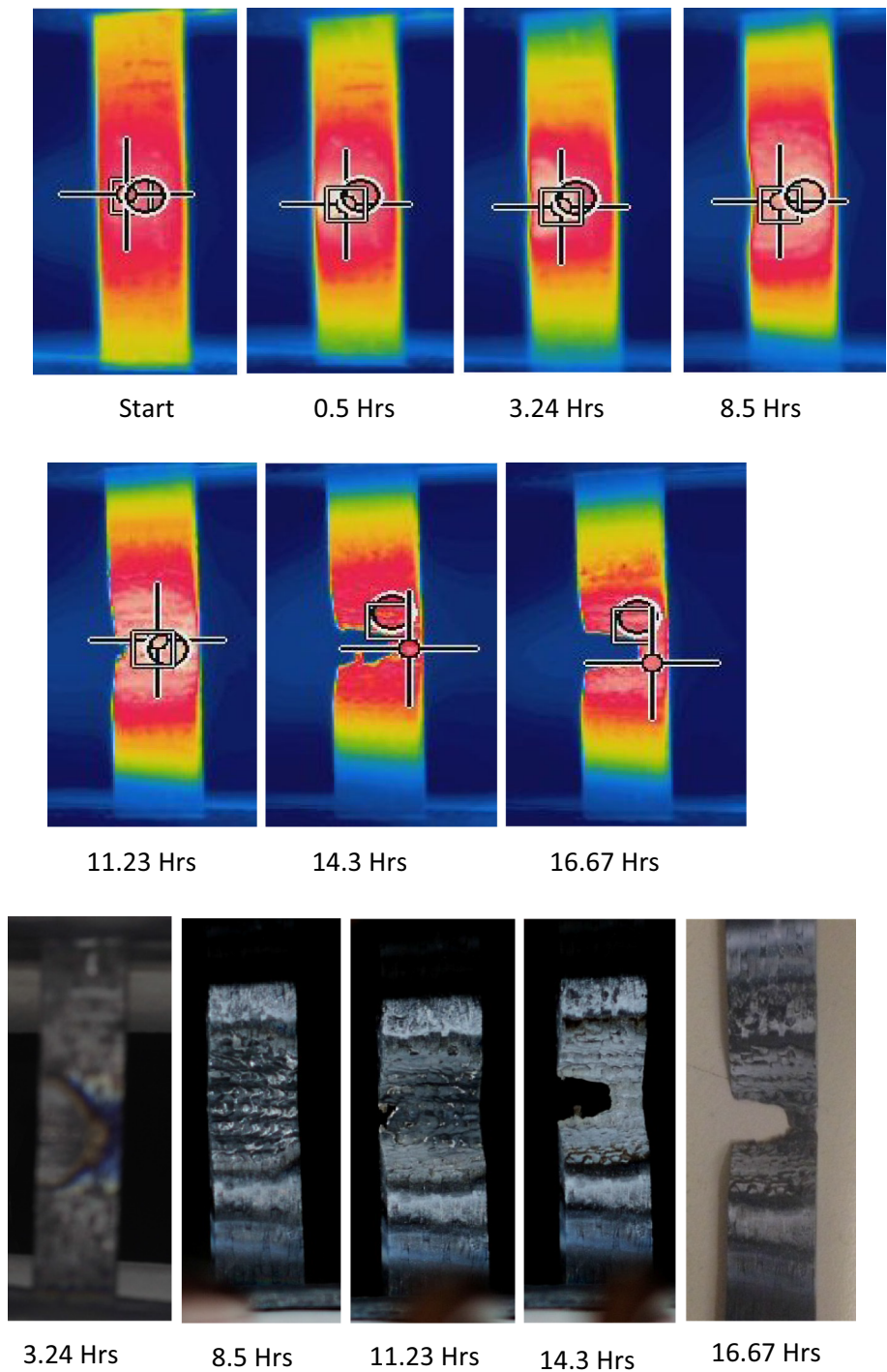
**Fig. 9** Material loss on a fractured specimen tested at 1480 °C and 80 MPa maximum stress

Fig. 10 IR images (*top two rows*) of width face along with erosion along thickness (*bottom row*) of specimen tested at 1480 °C with no load



The permeation of O₂ varies linearly with the partial pressure of O₂ and H₂O. The volatilization of SiO₂ scale varies with the square of the partial pressure of H₂O. The velocity of the flow over the material affects the rate of gas diffusion into the material controlling the rate of recession as well. A computer-based model has been developed to

predict the recession rate of SiC, which was used to estimate the recession rate of the present set of CMC specimens by Parthasarthy at Air Force Research Laboratory, Wright-Patterson AFB. The computer model was based on the previous studies [26, 27]. The conditions that were input into the model were a temperature of 1480 °C, a gas composition of 14 % O₂ and 35 % H₂O, a flame velocity of 100 m/s, and a pressure of 5 atm. With these conditions,

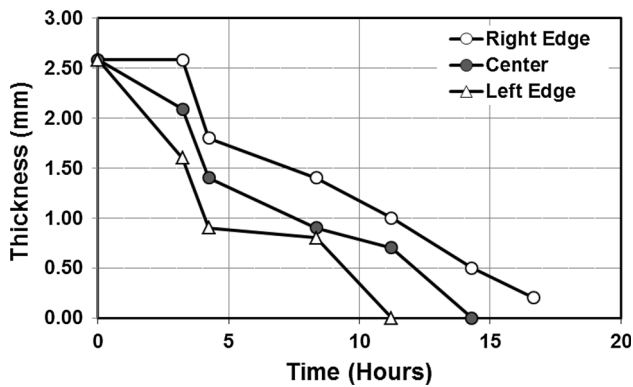


Fig. 11 Reduction in thickness with combustion exposure time of specimen tested at 1480 °C with no load

the model predicted a recession rate of 3.5 $\mu\text{m}/\text{h}$ for pure SiC, and SiO₂ scale evaporates as fast as the material oxidizes, and reaches a steady state thickness of 0.8 μm . The predicted recession rate of 3.5 $\mu\text{m}/\text{h}$ gas was considerably lower than the experimental value of 0.18 mm/h. This difference is due the fact that the model is based on the idealized condition, i.e., the analysis is for a dense SiC, whereas the CMC material of this study was porous and contained non-homogeneous SiC material. Further, the current analysis is not able to capture fully all test phenomena of this study such as high velocity combustion flame that would also cause significant erosion of the material in addition to oxidation phenomenon captured by the analytical model. This suggests that erosion from a high velocity combustion flame would be much larger than other effects.

Residual strength

Specimens, which survived 25 h (90,000 fatigue cycles) under combustion fatigue, were tested under the monotonic tensile condition to measure the residual stress–strain relationship. These data were then compared with the ultimate strength at room temperature of the as-received material. The as-received tension data were provided by Rolls-Royce High Temperature Composites. These comparisons are shown in Fig. 12, where three stress–strain relationships are shown for as-received, after combustion fatigue test at 1250 °C, and after combustion fatigue test at 1350 °C. The ultimate tensile strength reduced by 70 and 35 % for 1250 and 1350 °C specimens approximately in comparison to the initial values, respectively, while the reduction in Young’s modulus was about 62 % at both temperatures. It should be noted that 1250 °C specimen was tested at a higher stress level of 125 MPa than stress level of 88 MPa for 1350 °C specimen. Further, 1250 °C specimen was tested at a stress level which was much

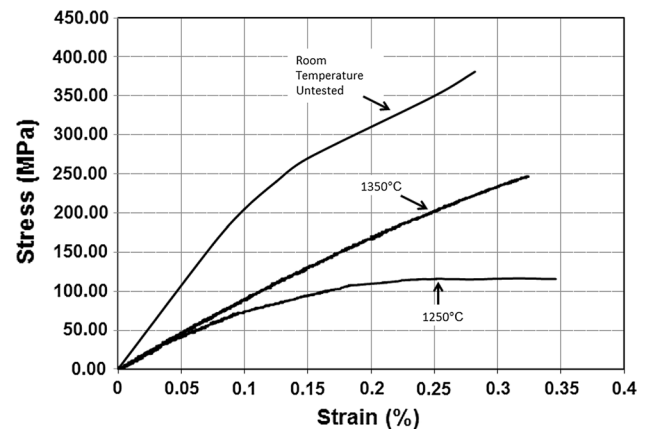


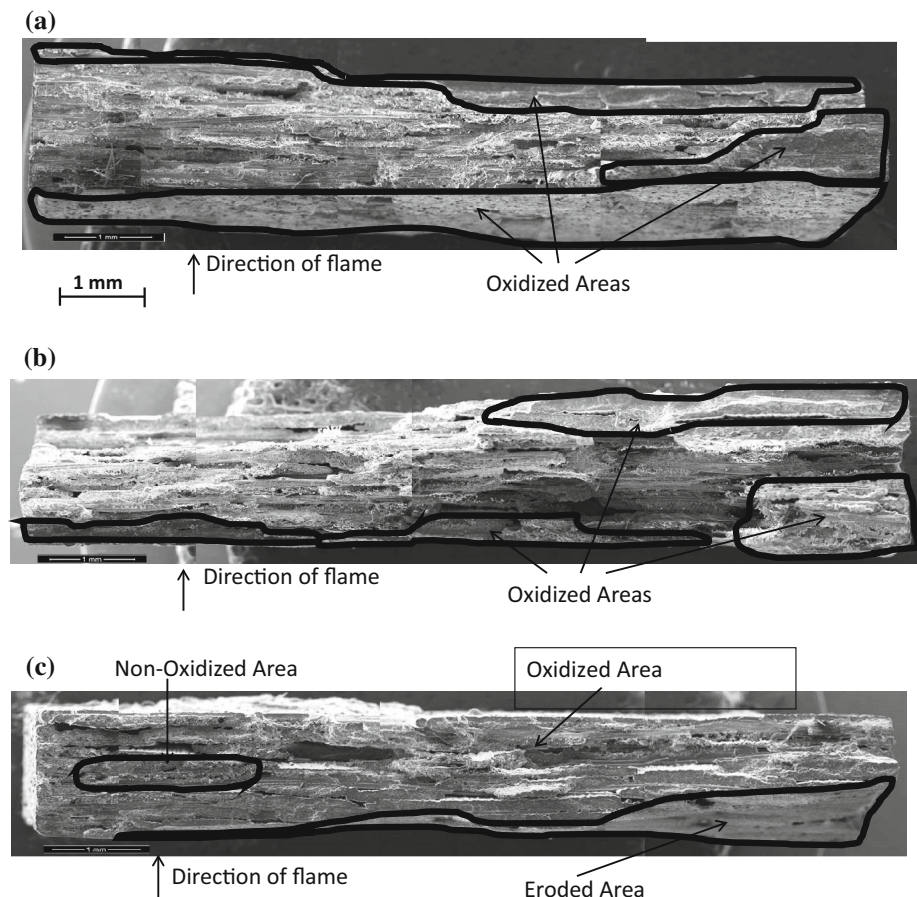
Fig. 12 Tensile stress–strain relationship before and after 1250 and 1350 °C combustion fatigue test

higher than the proportional limit of 100 MPa (Fig. 5), while 1350 °C specimen was tested at stress level lower than the proportional limit. Thus, it is expected that 1250 °C specimen would develop considerable internal damage just after the first cycle while it was not be the case in 1350 °C. Thus, the residual strength is expected to be lower in 1250 °C specimen than in 1350 °C specimen as observed. In other words, the reduction would depend not only on the test temperature but also on the applied stress level.

Damage mechanism

The Scanning Electron Microscopy (SEM) images of fracture surfaces of three specimens, one representative from three test temperatures (1250, 1350, and 1480 °C), are shown in Fig. 13. These fracture surfaces show damage and failure mechanisms. Two distinct regions are present on fracture surface of all specimens, which are identified in the figure. One region has a relatively planar fracture with little or no fiber pull-out, and this is identified as “oxidized.” The embrittlement occurs in SiC/SiC CMCs due to oxidation of BN interface under the oxidizing combustion environment as elaborated in the introduction. This phenomenon has been observed in previous combustion fatigue studies with SiC/SiC systems [22–24]. The other region of the fracture surface showing typical fiber pull-out with no apparent oxidative features is referred to as “non-oxidized.” The latter region shows the failure due to the inability of the remaining fibers to sustain the applied load resulting in their rapid failure. Figure 14 shows the details of these regions. Figure 14a shows a magnified view of the fracture surface from a specimen tested at 1250 °C which shows both “oxidized” and “non-oxidized” regions. In the oxidized region, fibers and matrix are fused together due to the formation of borosilicate glass

Fig. 13 - SEM Images of fracture surface at three different test temperatures: **a** 1250 °C, **b** 1350 °C, and **c** 1480 °C



from the interaction of BN interphase with moisture [22–24]. Figure 14b shows a magnified view of the fracture surface from a specimen tested at 1480 °C which shows only “oxidized” region. Similar embrittlement behavior was present from maximum to minimum test temperatures of the present study. On the other hand, typical fiber pull-out, as seen in brittle CMCs, is evident in the non-oxidized region, Fig. 14a. Oxidiaztion due to the combustion environment occurred near the surface on both the flame side and backside of the specimen, but more on the flame side. In the case of specimens tested at 1480 °C, there was a third region on the fracture surface as shown in Fig. 13, and this is marked as “eroded.” Material erosion occurred in this region as mentioned earlier. A magnified view in this region is shown in Fig. 15 where erosion of material from the volatilization of BN fiber coating and surrounding materials is evident, as discussed earlier. The volatilization was also present away from the fracture surface as shown in Fig. 16 which shows the polished sections away from the fracture surface of a tested specimen at 1480 °C. Figure 16a shows the longitudinal section where the combustion gases caused volatilization of the BN coating leaving no fiber–matrix interface. This was due to

stovepiping phenomenon i.e., gases from combustion traveled along the fiber length. Figure 16b shows the transverse section of the same specimen where volatilization of the BN fiber coating along with formation of borosilicate glass around the fibers is evident.

General discussion

The material did not show the material loss due to the combustion environment up to 1350 °C and survived 25 h of fatigue with the applied maximum stress of 51 and 33 % of the ultimate tensile strength under combustion at 1250 and 1350 °C, respectively. At the test temperature of 1480 °C, the material did not survive more than 17 h of exposure to the combustion environment even without any load. As mentioned earlier, the primary reason for the failures at 1480 °C was the material loss. The combustion provides an environment of high temperature gases and water vapor which causes oxidation to start. Then, the high velocity flame present in this environment introduces erosion of the material. The make-up of the material contributes this degradation. The weave pattern of the fibers of CMC would produce uneven surface with local valleys and

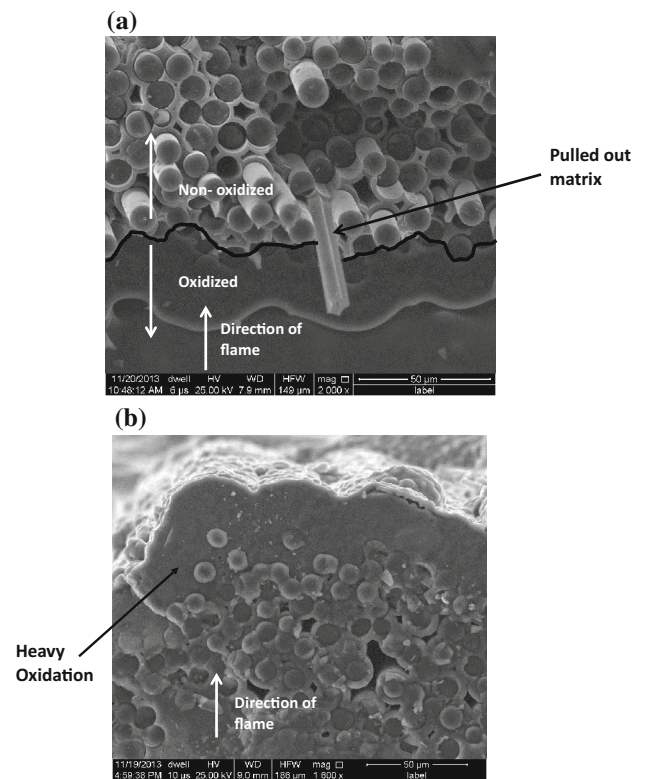


Fig. 14 Magnified view of fracture surface: **a** 1250 °C and **b** 1480 °C

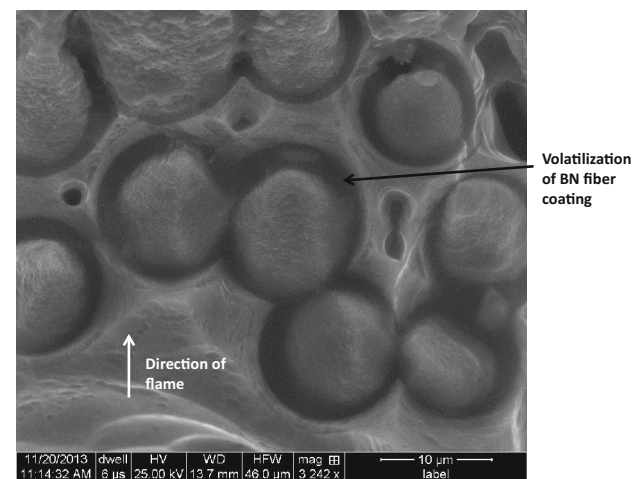


Fig. 15 Erosion of material from volatilization of BN fiber coating and surrounding materials in specimen tested at 1480 °C

crests on the surface. In the valley regions, combustion gases would pool and increase the temperature locally. There was a localized increase in temperature up to 1650 °C over an area of about 0.05 mm × 0.05 mm, where material loss began due to volatilization. On the other hand, such temperature rise on localized hot-spots was 1300 and 1420 °C in the tests with an average test

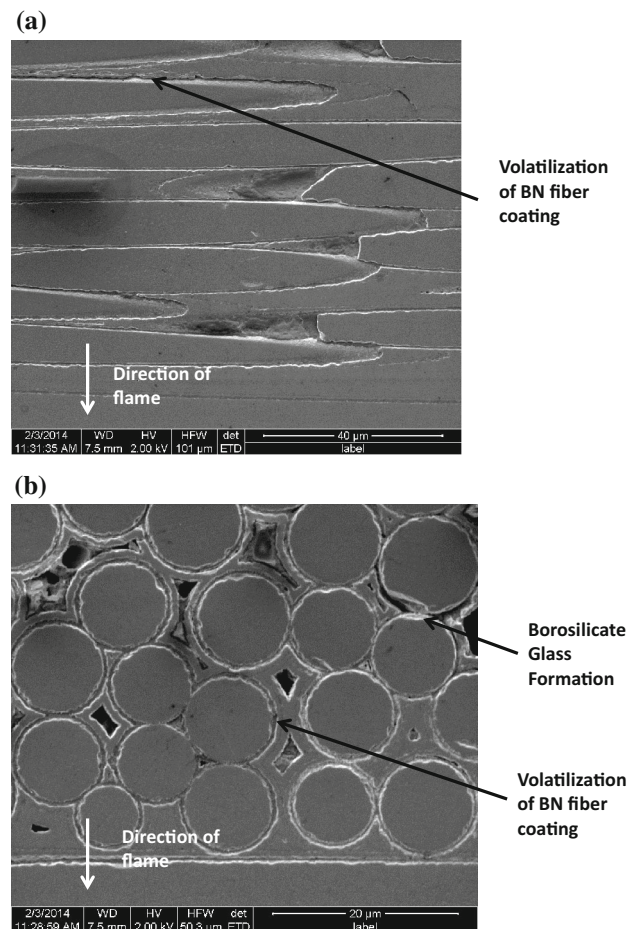


Fig. 16 Polished sections of specimen tested at 1480 °C: **a** longitudinal section and **b** transverse section

temperature of 1250 and 1350 °C, respectively. Further, these localized hot-spots were relatively fewer in 1250 and 1350 °C test than those at 1480 °C test. Thus, changes to the surface texture would prevent development of the hot-spots, and hence the CMC would possibly achieve run-out at the average temperature of 1480 °C in the combustion environment. In other words, the tested CMC has a potential to withstand the average temperature of 1480 °C or more in the combustion environment if appropriate environmental barrier coating(s) are utilized which will be the focus of the future investigation.

Conclusions

Sylramic-iBN/BN/CVI SiC CMC was investigated under tension–tension fatigue using a burner rig facility which simulated combined load and combustion conditions of hot-section components of gas turbine engines such as turbine blades and vanes. Fatigue tests were performed with this facility at stress ratio of 0.1 and frequency of 1 Hz

to establish fatigue life data. The combustion environment was created using a high-velocity oxygen fuel gun, which impinged the flame directly on the one side of specimen when it was subjected to cyclic load. The flame-impinged surface of the specimen was heated to the average temperature of 1250, 1350, and 1480 °C. The CMC achieved a run-out of 25 h at 46 and 33 % of the ultimate tensile strength under combustion at 1250 and 1350 °C, respectively. Run-out was not achieved at 1480 °C due to erosion and degradation of the material. At 1480 °C, significant loss of material was observed leading to considerable decrease in fatigue life compared to 1250 and 1350 °C. Microscopic analysis showed that the oxidation, i.e., embrittlement of material due to the combustion environment occurred near the surface on both flame side and backside of the specimen, but more on the flame side. The fracture surfaces showed regions with oxide formations which covered matrix and/or fibers, oxides filled of the fiber/matrix interphase, or both leading to embrittlement of CMC. At 1480 °C, significant loss of material was observed leading to considerable decrease in fatigue life compared to 1250 and 1350 °C. It appears that the make-up of the material, i.e., uneven surface texture contributed to the increased temperature locally which contributed to the erosion and degradation of the material. The CMC can potentially withstand average temperature of 1480 °C in the combustion fatigue environment with appropriate modification of the surface texture such as with the use of environmental barrier coating(s).

References

- Schmidt S, Beyer S, Knabe H, Immich H, Meistring R, Gessler A (2004) Advanced ceramic matrix composite materials for current and future propulsion system applications. *Acta Astronaut* 55:409–420
- DiCarlo JA, Roode MV (2006) Ceramic composite development for gas turbine hot section components. In: *Proceedings of the ASME Turbo Expo: Power for Land, Sea and Air*, vol. 2, pp. 221–231
- Haynes JA, Lance MJ, Cooley KM, Ferber MK, Lowden RA, Stinton DP (2000) CVD multiple coating in high-temperature, high-pressure air-H₂O. *J Am Ceram Soc* 83–3:657–659
- Opila EJ, Hann RE (1997) Paralineer oxidation of SiC in water vapor. *J Am Ceram Soc* 80–1:197–205
- Opila EJ (1994) Oxidation kinetics of chemically vapor deposited silicon carbide in wet oxygen. *J Am Ceram Soc* 77–3:730–736
- Opila EJ (1999) Variation of oxidation rate of silicon carbide with water-vapor pressure. *J Am Ceram Soc* 82–31:625–636
- Jacobson NS (1993) Corrosion of silicon-based ceramics in combustion environments. *J Am Ceram Soc* 76–1:3–28
- Tomas-Ogboji L (1998) A pervasive model of oxidation degradation in a SiC-SiC composite. *J Am Ceram Soc* 82–11:2777–2784
- More KL, Tortorelli PF, Lin HT, Lara-Curzio E, Lowden RA (1998) Degradation mechanisms of BN interfaces in SiC/SiC composites in oxygen- and water containing environments. *Electrochem Soc Proc* 98–99:382–395
- Cofer GC, Economy J (1995) Oxidative and hydrolytic stability of boron nitride—a new approach to improving the oxidation resistance of carbonaceous structures. *Carbon* 33–4:389–395
- Matsuda T (1989) Stability to moisture for chemically vapour-deposited boron nitride. *J Mater Sci* 24:2353–2357
- Morscher GN, Bryant D, Tressler RE (1997) Environmental durability of different BN interphases (for SiC/SiC) in H₂O-containing atmospheres at intermediate temperatures. *Ceram Eng Sci Proc* 18–3:525–533
- Tomas-Ogboji L (1998) Degradation of SiC/BN/SiC composite in the burner rig. *Ceram Eng Sci Proc* 19–4:257–264
- Jacobson N, Farmer S, Moore A, Sayir H (1999) High-temperature oxidation of boron nitride: I. Monolithic boron nitride. *J Am Ceram Soc* 82–2:393–398
- Jacobson NS, Morscher GN, Bryant DR, Tressler RE (1999) High-temperature oxidation of boron nitride: II. Boron nitride layers in composites. *J Am Ceram Soc* 82–6:1473–1482
- LaRochelle KJ, Mall S (2003) Temperature and moisture effects upon stress rupture life of Syl-iBN/BN/SiC composites. *Ceram Eng Sci Proc* 24–4:459–464
- Mall S, LaRochelle KJ (2006) Fatigue and stress-rupture behaviors of SiC/SiC composite under humid environment at elevated temperature. *Compos Sci Technol* 66:2925–2934
- Mall S (2005) Effects of moisture on fatigue behavior of SiC/SiC composite at elevated temperature. *Mater Sci Eng A* 412:165–170
- Ogboji LUJT, Yun HM, DiCarlo J (2002) Effect of adventitious carbon on the environmental degradation of SiC/BN/SiC composites. *NASA/TM* 2002-211494
- Ogboji LUJT (2000) Degradation of a SiC/SiC composite in the burner rig: investigation by fractography. *Mater High Temp* 17–2:369–372
- Richardson GY, Lei CS, Singh RN (2004) Mechanical properties of ceramic matrix composites exposed to rig tests. *Ceram Eng Sci Proc* 25–4:153–159
- Kim TT, Mall S, Zawada LP (2009) Fatigue characterization of a melt-infiltrated woven Hi-NiC-S/BN/SiC ceramic matrix composite (CMC) using a unique combustion test facility. *Ceram Trans* 179:103–116
- Kim TT, Mall S, Zawada LP, Jefferson G (2010) Simultaneous fatigue and combustion exposure of a SiC/SiC ceramic matrix composite. *J Compos Mater* 44–25:2991–3016
- Kim TT, Mall S, Zawada LP (2011) Fatigue behavior of Hi-NiC-S/BN/SiC ceramic matrix composites in a combustion environment. *Int J Appl Ceram Technol* 8–2:261–272
- Mall S, Nye AR, Jefferson G (2012) Tension-tension fatigue behavior of NextelTM720/Alumina under combustion environment. *Int J Appl Ceram Technol* 9–1:159–171
- Robinson RC, Smialek JL (1999) SiC recession caused by SiO₂ scale volatility under combustion conditions: I. Experimental results and empirical model. *J Am Ceram Soc* 82–7:1817–1825
- Opila EJ, Smialek JL, Robinson RC, Fox DS, Jacobson NS (1999) SiC recession caused by SiO₂ scale volatility under combustion conditions: II. Thermodynamics and gaseous-diffusion model. *J Am Ceram Soc* 82–7:1826–1834